Nuclear Inst. and Methods in Physics Research, A 954 (2020) 161723

Contents lists available at ScienceDirect

Nuclear Inst. and Methods in Physics Research, A

journal homepage: www.elsevier.com/locate/nima

LuAG ceramic scintillators for future HEP experiments

Chen Hu [a], Jiang Li [b], Fan Yang [a,c], Benxue Jiang [d], Liyuan Zhang [a], Ren-Yuan Zhu [a,*]

[a] 256-48, HEP, California Institute of Technology, Pasadena, CA 91125, USA
[b] Shanghai Institute of Ceramics, 1295 Dingxi Rd, Shanghai, 200050, China
[c] Nankai University, 94 Weijin Rd, Tianjin, 300071, China
[d] Shanghai Institute of Optics and Fine Mechanics, 390 Qinghe Rd, Shanghai, 201800, China

ARTICLE INFO

Keywords:
LuAG ceramics
Radiation hardness
Slow component suppressed
Co-doping

ABSTRACT

Because of its bright and fast scintillation cerium-doped $Lu_3Al_5O_{12}$ (LuAG:Ce) crystals have attracted an interest in the high energy physics community. Compared to inorganic crystals, fabrication of ceramic scintillators features with a lower temperature and a more effective use of raw materials, thus promising cost-effective inorganic scintillators. Our investigations revealed excellent radiation hardness of LuAG:Ce ceramics in both transmittance and light output against an ionization dose up to 200 Mrad and a proton fluence up to 3×10^{14} p/cm^2. We also investigated light output and decay kinetics for LuAG:Ce ceramics with different Ce doping levels and various co-dopings. The results show increased light output and slow scintillation component when the Ce doping level increases. Ca^{2+} co-doping is found effective in suppressing slow scintillation component in LuAG:Ce ceramics. We also discuss the status of LuAG ceramic scintillators and future development plan.

Contents

1. Introduction

Because of their relative high density of 6.73 g/cm^3, fast scintillation with a decay time of about 50 ns and a high light output of 26,000 photons/MeV, cerium-doped $Lu_3Al_5O_{12}$ aluminum garnet crystals (LuAG:Ce) have attracted an interest in the high energy physics (HEP) community [1]. The low segregation coefficient of Ce^{3+} ions in LuAG lattice and the Lu_{Al} antisite defects (Lu ions at the octahedral Al site) formed during the high temperature process, however, seriously compromise LuAG:Ce crystal's performance. Researches [2–5] have, therefore, been focused on their cost-effective ceramic counterpart. Compared to crystal scintillators, the fabrication process of ceramic scintillators features with a lower temperature, a uniform doping distribution and a more effective use of raw materials. LuAG:Ce ceramics thus is a cost-effective alternative for LYSO:Ce crystals for the proposed shashlik sampling calorimeter detector concept for future HEP experiments [6]. Fig. 1 shows the LYSO/W shashlik calorimeter concept consisting of 1.5 mm LYSO plates as active material interleaved with 2.5 mm tungsten plates as absorbers, four quartz capillaries as wavelength shifters, and one quartz leaky fiber for injection of monitoring light. A crucial issue for such an application is the radiation damage in a severe radiation environment. With 5×10^{34} cm^{-2} s^{-1} luminosity and 3000 fb^{-1} integrated luminosity, the HL-LHC will present a very severe radiation environment, where up to 130 Mrad ionization dose, 3×10^{14} charged hadrons/cm^2 and 5×10^{15} n/cm^2 are expected [7].

In this investigation, optical and scintillation properties of LuAG:Ce ceramic plates, such as photo-luminescence (PL), x-ray excited luminescence (XEL), transmittance, pulse height spectrum (PHS), light output

* Corresponding author.
E-mail address: zhu@hep.caltech.edu (R.-Y. Zhu).

https://doi.org/10.1016/j.nima.2018.12.038
Received 20 July 2018; Received in revised form 5 December 2018; Accepted 10 December 2018
Available online 18 December 2018
0168-9002/

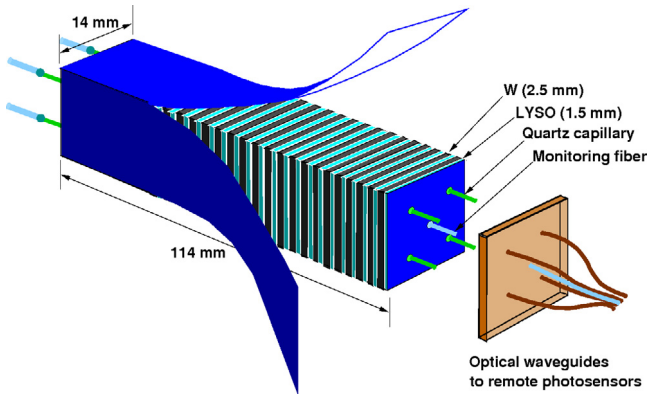

Fig. 1. A schematic showing a LYSO/W shashlik sampling calorimeter concept.

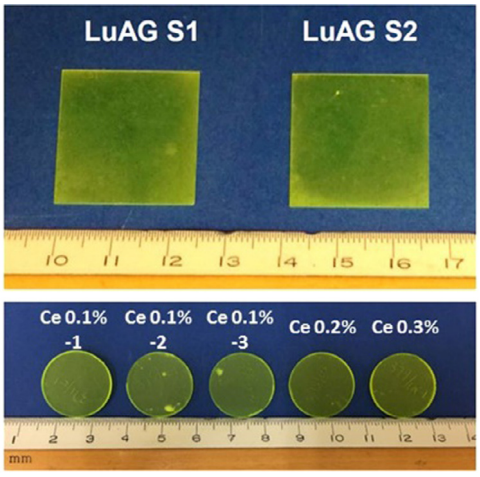

Fig. 2. LuAG:Ce ceramic plates of 25 × 25 × 0.4 (top) and Φ19 × 1.5 mm^3 with different Ce dopings (bottom).

(LO) and decay kinetics, were measured in the Caltech HEP crystal lab before and after irradiations by gamma-rays and 800 MeV protons. The results of this investigation show that LuAG:Ce ceramics have excellent radiation hardness against an ionization dose up to 200 Mrad and a proton fluences up to 3×10^{14} p/cm^2. A slow scintillation component with a decay time of about 1 μs, however, was also found in LuAG:Ce ceramic samples. We report also an investigation on slow component suppression in LuAG:Ce ceramics by varying Ce doping levels and by introducing various co-dopings. Status of LuAG:Ce ceramic scintillators and future development plan are also discussed.

2. Samples and measurements

Fig. 2 shows two LuAG:Ce square ceramic plates with a dimension of 25 × 25 × 0.4 mm^3(top) and five round plates of Φ19 × 1.5 mm^3 (bottom) with cerium doping levels of 0.1, 0.2, and 0.3 mol%, sintered at Shanghai Institute of Ceramics (SIC) with no additional polishing. In addition to these samples, Table 1 lists LuAG:Ce samples of Φ14 × 1 mm^3 co-doped with Li^+, Ca^{2+}, Mg^{2+}, Li^+/Mg^{2+} and Ca^{2+}/Mg^{2+} sintered at SIC, and samples of Φ17 × 1 mm^3 with Ca^{2+} and Ca^{2+}/Mg^{2+} co-doping sintered at Shanghai Institute of Optics and Fine Mechanics (SIOM). These samples were mirror-polished on large surfaces.

PL and time-resolved PL were measured by using an Edinburgh Instruments FLS 920 fluorescence spectrometer. For the XEL measurements, samples were placed in the sample compartment of a HITACHI F-4500 spectrophotometer. X-rays generated by an Amptek Eclipse-III x-ray tube were used to excite the sample. Transmittance was measured

Table 1
Other LuAG:Ce ceramic samples.

Co-dopants	Vendors	Dimension (mm^3)	Numbers
Li^+	SIC	Φ14 × 2	2
Mg^{2+}	SIC	Φ14 × 1	11
Ca^{2+}	SIC	Φ14 × 1	10
Li^+, Mg^{2+}	SIC	Φ14 × 2	6
Ca^{2+}, Mg^{2+}	SIC	Φ14 × 1	3
Ca^{2+}	SIOM	Φ17 × 1	5
Ca^{2+}, Mg^{2+}	SIOM	Φ17 × 1	5

by using a PerkinElmer Lambda 950 spectrophotometer with 0.15% precision. LO was measured by using a Hamamatsu R1306 PMT with a grease coupling between the sample and the PMT for 0.662 MeV γ-rays from a ^{137}Cs source with self-trigger and 0.511 MeV γ-rays from a ^{22}Na source with a coincidence trigger, respectively. The systematic uncertainty of the LO measurement is about 1%.

Both samples S1 and S2 were irradiated by gamma-rays and protons. The sample S1 was irradiated by ^{60}Co gamma-rays in several steps to reach 220 Mrad at the total ionization dose facility of the Jet Propulsion Laboratory, and was followed by irradiation by 800 MeV protons with a fluence up to 3×10^{14} p/cm^2 at the Weapons Neutron Research facility of Los Alamos Neutron Science Center (LANSCE). The ceramic plate S2 was irradiated by ^{137}Cs gamma-rays to 1 Mrad at Caltech and up to 200 Mrad at the Sandia Gamma Irradiation Facility.

3. Experimental results

3.1. Basic scintillation performance

Figs. 3 and 4 show PL and XEL spectra respectively for LuAG:Ce ceramics S1 and S2. Consistent Ce^{3+} peaks at about 500 nm were observed in both PL and XEL spectra. Two broad excitation bands peaked at 350 and 450 nm are attributed to the Ce 4f-5d$_2$ and 4f-5d$_1$ transition respectively. The overall asymmetric emission band is due to the overlap of two emission bands from the transitions between the 5d level and two split 4f levels of Ce^{3+} ($^2F_{5/2}$, $^2F_{7/2}$). The large stokes shift between excitation and emission spectra indicates that the self-absorption due to Ce^{3+} is negligible.

Fig. 5 shows the transmittance spectra measured along 0.4 mm (solid lines) together with the emission spectrum (dashed lines) and the numerical values of the emission weighted longitudinal transmittance (EWLT) for S1 and S2. The two dips at 350 and 450 nm observed in the transmittance spectra are due to Ce^{3+} absorption, which are consistent with Ce^{3+} excitation bands in Fig. 3. No serious self-absorption was observed, which is consistent with the PL spectra. Because of the unpolished surfaces and scattering centers inside the ceramics, the EWLT values for both samples are lower than the theoretical limit of 84% calculated by taking into account multiple bouncing between two end surfaces and assuming no internal absorption [8].

Fig. 6 shows their PHS measured with an integration time of 200 ns. The LO of both samples exceeds 1400 p.e./MeV. The FWHM energy resolution is 19% for ^{137}Cs γ-rays.

Fig. 7 shows LO as a function of integration time for S1 and S2. In addition to the fast scintillation light with a decay time of about 50 ns due to the 5d-4f electric dipole allowed radiative transition of Ce^{3+}, a slow component with a decay time of about 1 μs is also observed in both samples. The fast to total ratio (F/T), defined as the ratio between the LO in 200 ns and the LO in 3000 ns, is 71% for both S1 and S2. Such a slow component would cause a pileup effect for HEP experiments with high event rate, so should be suppressed or eliminated.

LuAG:Ce single crystals samples show a LO in 3000 ns of 3730 p.e./MeV or 20,700 ph/MeV [9], and a fast component of about 47% of the total scintillation light within 1000 ns range [10]. Taking into account the different quantum efficiency values of the PMTs used in the LO measurement, the LuAG:Ce ceramic samples show a similar LO

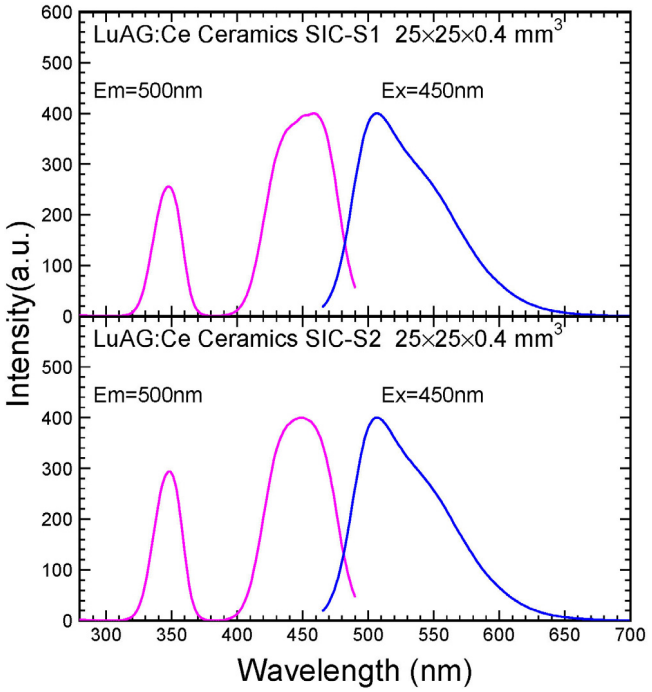

Fig. 3. Excitation (red) and PL (blue) spectra for the LuAG:Ce samples S1 and S2 . (For interpretation of the references to color in this figure legend, the reader is referred to the web version of this article.)

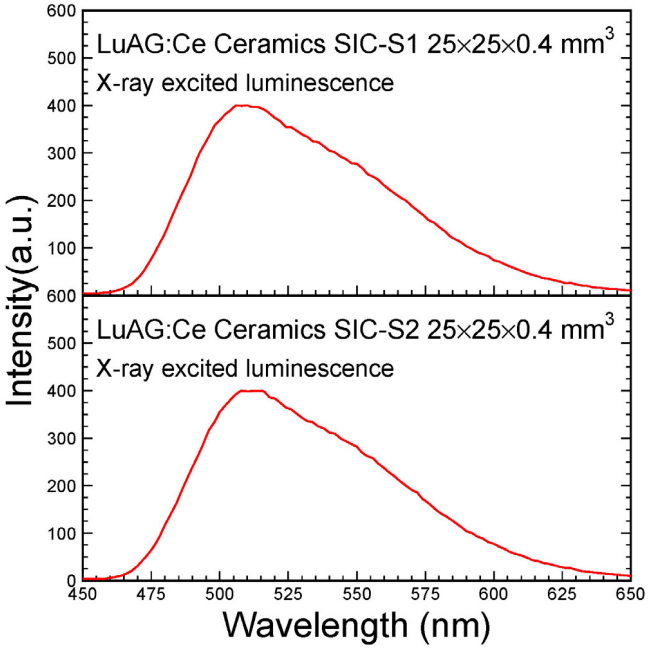

Fig. 4. XEL spectra for the LuAG:Ce samples S1 and S2.

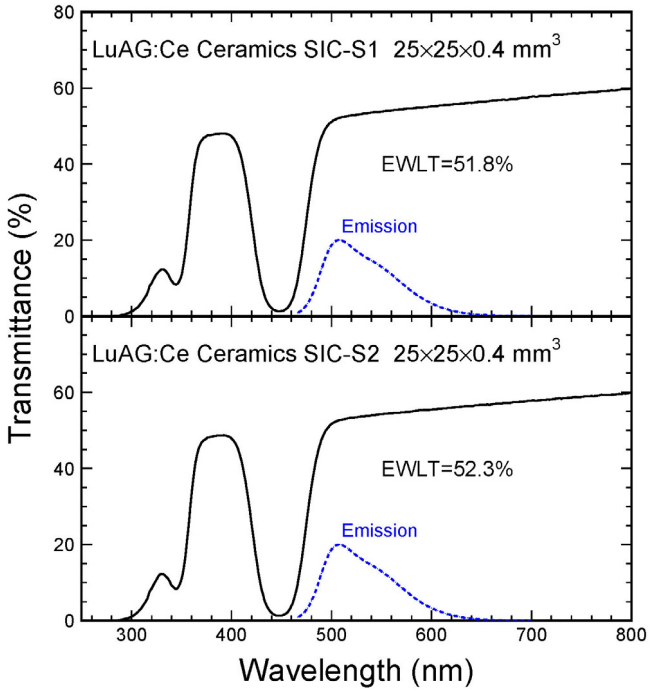

Fig. 5. Transmittance along 0.4 mm and emission for the LuAG:Ce samples S1 and S2.

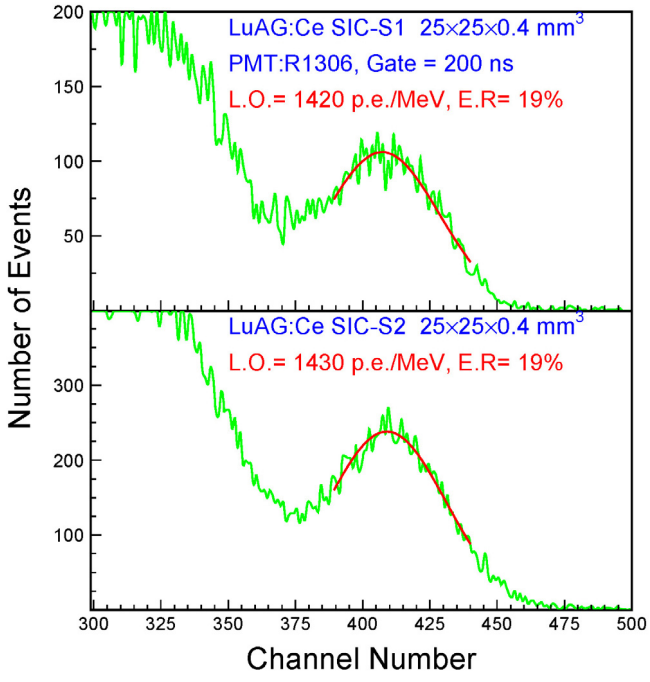

Fig. 6. PHS for the LuAG:Ce ceramic samples S1 and S2.

in 3000 ns of 2050 p.e./MeV or 20,500 ph/MeV, and a reduced slow component.

Fig. 8 shows PL decay profiles for S1 and S2 at 500 nm with 350 nm and 450 nm excitation. Also shown in the figure is the instrumental instrument response function (IRF). A single exponential function was used to fit the decay profile. A decay time of about 50 ns is extracted, which is consistent with the scintillation decay time observed in Fig. 7. The slow component with decay time of about 1 μs, however, is not shown in this plot because of limited time scale.

3.2. Radiation hardness of LuAG ceramics

Figs. 9 and 10 show transmittance and LO respectively for S1 (top) and S2 (bottom) before and after irradiations of up to 220 Mrad plus 2.94×10^{14} p/cm^2 by 800 MeV protons. It is interesting to note that both transmittance and LO show almost no degradation, indicating that LuAG ceramics have excellent radiation hardness against ionization dose and proton fluence.

Fig. 11 summarizes the values of the normalized EWLT (top) and LO (bottom) for LuAG:Ce plates S1 (dots) and S2 (triangles) as a function of

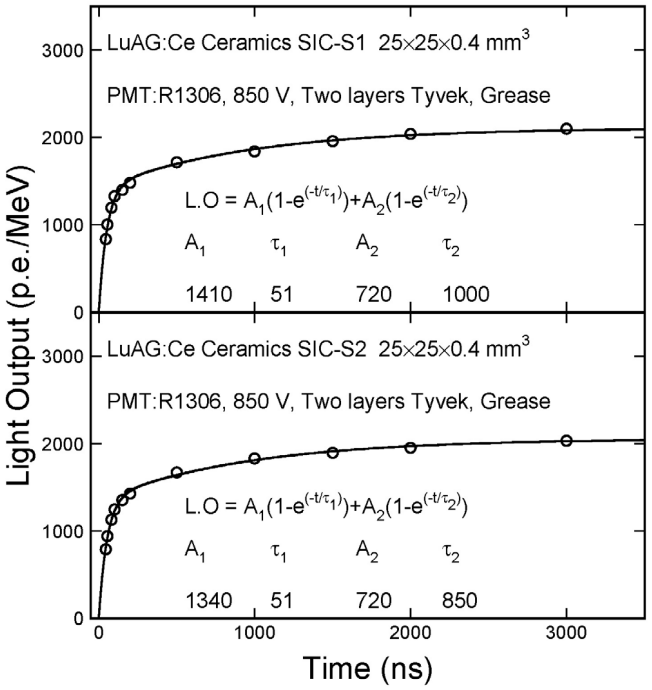

Fig. 7. LO and decay kinetics for the LuAG:Ce samples S1 and S2.

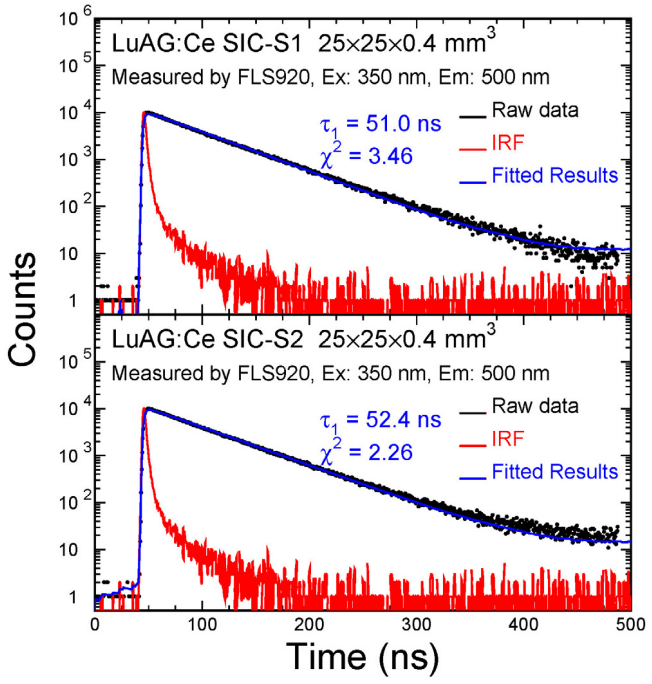

Fig. 8. PL decay profiles for the LuAG:Ce samples S1 and S2.

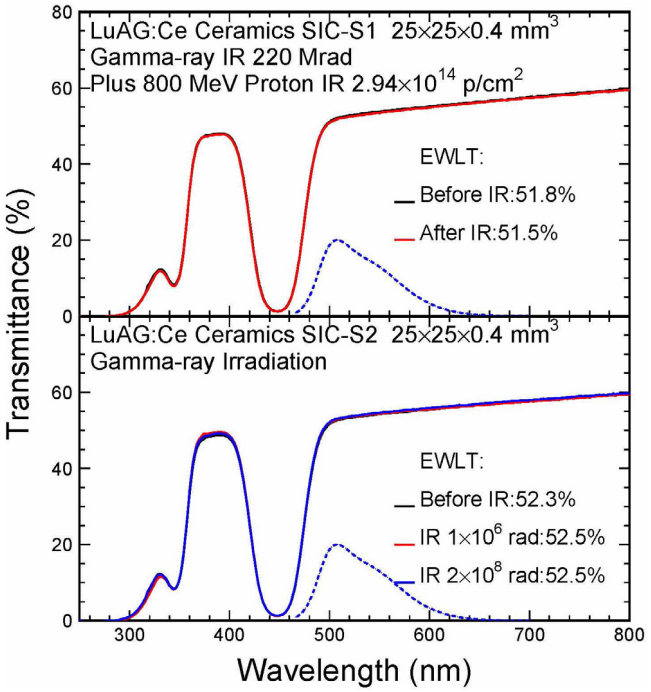

Fig. 9. Transmittance spectra for LuAG:Ce samples S1 and S2 before and after γ-ray and proton irradiations.

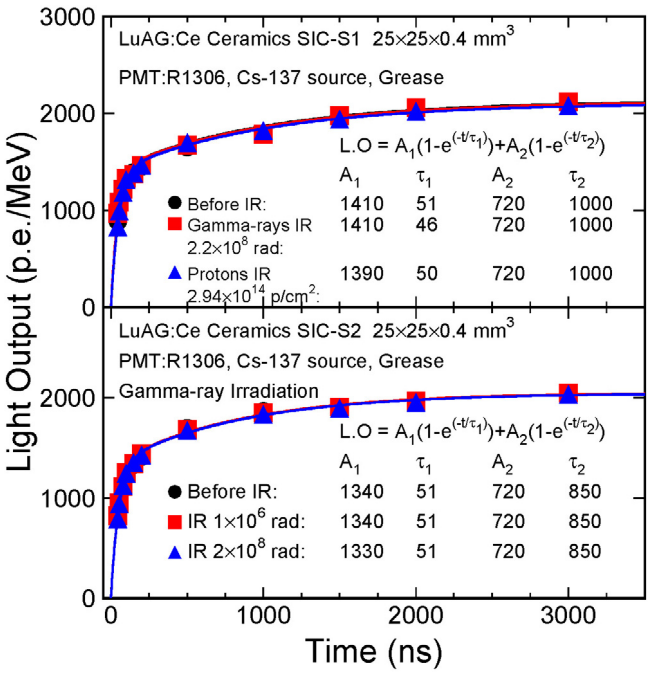

Fig. 10. LO and decay kinetics for LuAG:Ce samples S1 and S2 before and after γ-ray and proton irradiations.

the integrated dose. The excellent radiation hardness of LuAG samples indicates that this material is promising for future HEP experiments in a severe radiation environment, such as the HL-LHC.

3.3. Slow component and correlation to Ce concentration

Five LuAG:Ce plates with different Ce doping levels were sintered at SIC. Fig. 12 shows pulse height spectra with 200 ns integration time for five samples. Their light output increases from 1010 to 1400 p.e./MeV when the Ce concentration increases from 0.1 to 0.3%. The corresponding energy resolution improves from 24 to 17%.

Fig. 13 shows the light output as a function of integration time for these samples, showing a slow component with a decay time of about μs and the corresponding exponential fits. The light output of both the fast and slow component increases when the Ce concentration increases.

Fig. 14 shows correlations between the Ce concentration and the F/T ratio (top) and the LO in 200 ns (bottom) for five ceramic plates. While

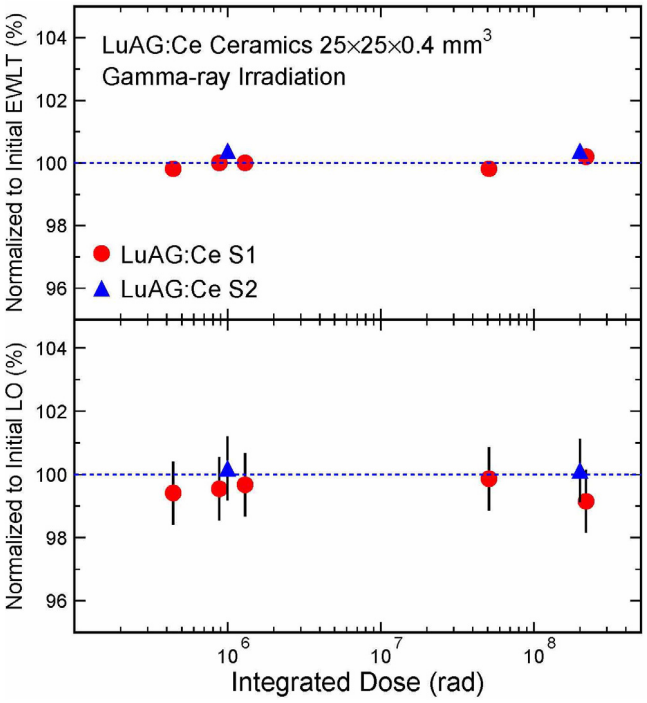

Fig. 11. Normalized EWLT (top) and LO (bottom) as a function of integrated dose for LuAG:Ce samples S1 and S2.

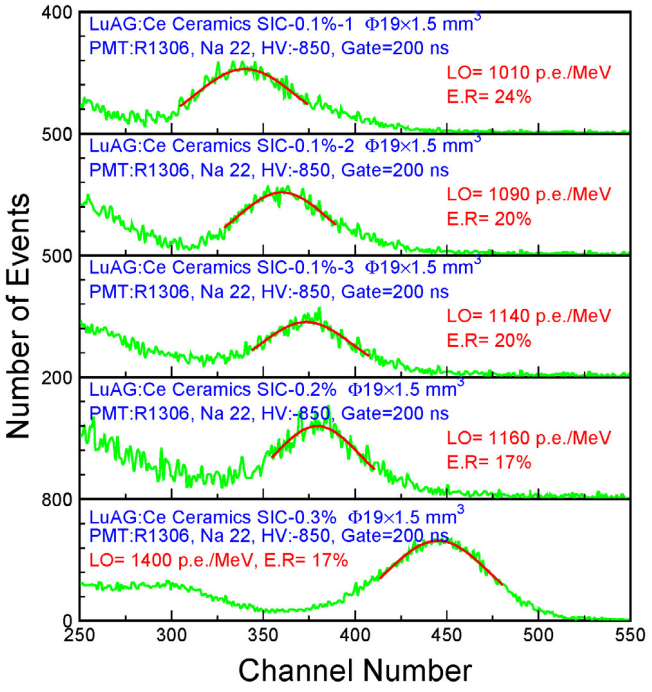

Fig. 12. PHS for five round LuAG:Ce ceramic samples with different Ce doping levels.

the F/T ratio decreases from 70% to 62% with the Ce doping concentration increased from 0.1 to 0.3 mol%, the LO in 200 ns increases from 1100 to 1400 p.e./MeV. This result indicates that further optimization of the Ce concentration is needed to find the best compromise between the F/T ratio and the LO.

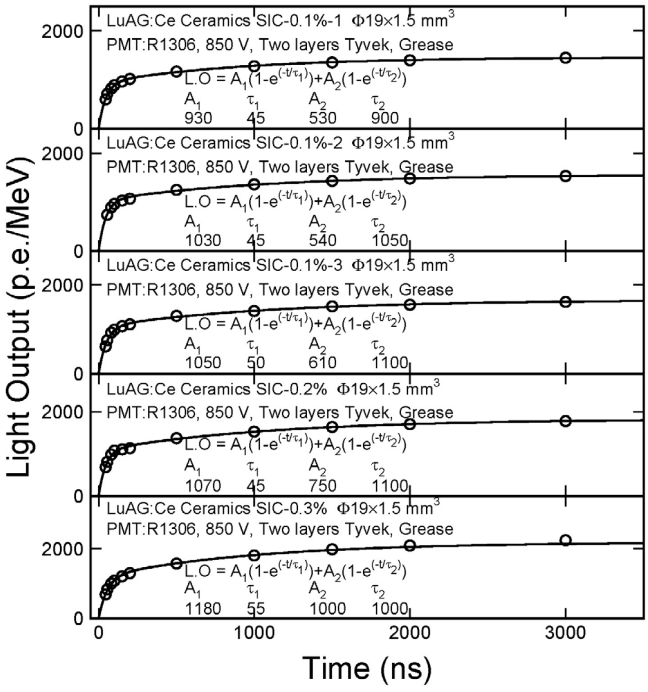

Fig. 13. LO and decay kinetics for five round LuAG:Ce ceramic samples with different Ce doping levels.

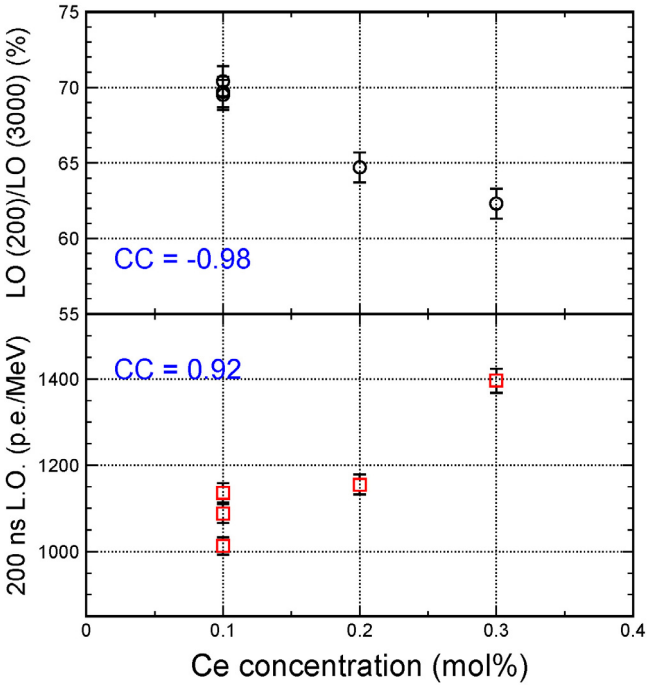

Fig. 14. Correlation between the Ce concentration and the F/T ratio (top) and the LO in 200 ns gate (bottom).

3.4. Slow component suppressed by co-doping

We also investigated slow suppression by co-doping. Figs. 15 and 16 show the LO and decay kinetics for LuAG:Ce ceramics co-doped with Mg^{2+} and Ca^{2+}, respectively. With Mg^{2+} co-doping, the F/T ratio improves to 74%, and the LO in 200 ns gate also increases to 1500 p.e./MeV. Compared with the Mg^{2+} co-doped samples, LuAG:Ce,Ca ceramics show a better F/T ratio up to 90%, but a reduced LO in 200 ns

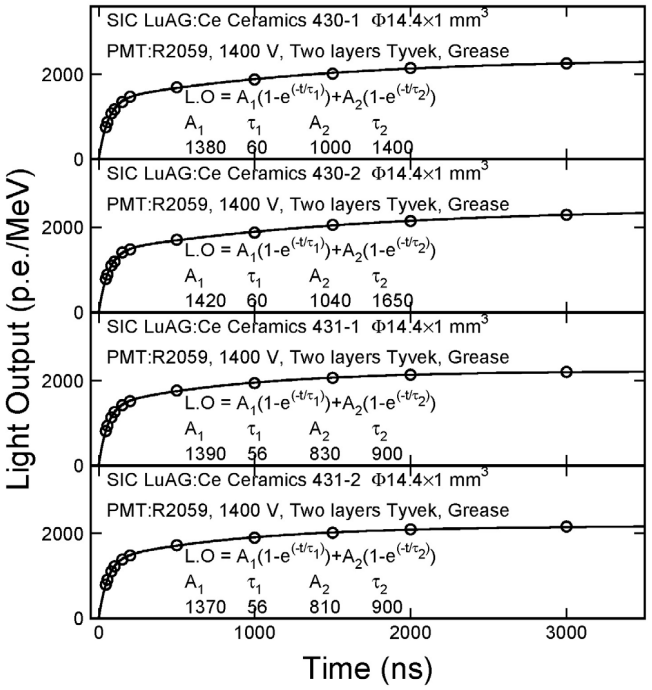

Fig. 15. LO and decay kinetics for four Mg^{2+} co-doped LuAG:Ce samples.

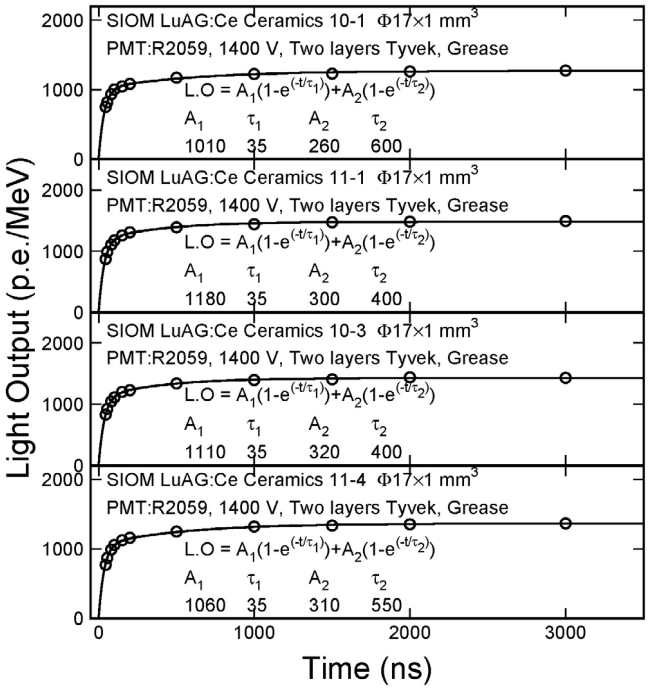

Fig. 16. LO and decay kinetics for four Ca^{2+} co-doped LuAG:Ce samples.

gate of about 1200 p.e./MeV. Fig. 17 shows the relationship between LO in 200 ns gate and LO in 3000 ns gate for LuAG:Ce ceramics with various mono- and divalent co-dopings. The four blue dash lines with different slopes are the F/T ratios from 60% to 90%. The LuAG:Ce ceramics without co-doping (black dots) show an F/T ratio of 62% and a LO in 200 ns of 1300 p.e./MeV. The effect of co-doping can be summarized as follows. Li^{+} co-doping reduces both the F/T ratio and the LO of 200 ns gate; Mg^{2+} co-doping improves the F/T ratio and shows the highest LO in 200 ns gate; and Ca^{2+} co-doping shows the highest F/T ratio of about 90%.

4. Conclusion

LuAG:Ce ceramics show an emission peaked at 500 nm with no self-absorption. Their emission has a fast decay time of 50 ns and a slow component with decay time of about 1 μs. Their light output is about 1400 p.e./MeV. Correlations are observed between the Ce concentration and the F/T ratio and light output in 200 ns.

LuAG:Ce ceramics are found to have excellent radiation hardness against an ionization dose up to 220 Mrad and a proton fluence up to 3×10^{14} p/cm^2. This material thus is promising for future HEP experiments to be operated in severe radiation environment, such as the HL-LHC.

Mono- and divalent co-dopants are investigated to suppress the slow component in LuAG:Ce. While the Mg^{2+} co-doping shows the highest LO of 200 ns gate, the F/T ratio reaches 90% for Ca^{2+} co-doped ceramics. Further development will continue to develop Ca co-doped LuAG:Ce ceramics and LuAG:Pr ceramics.

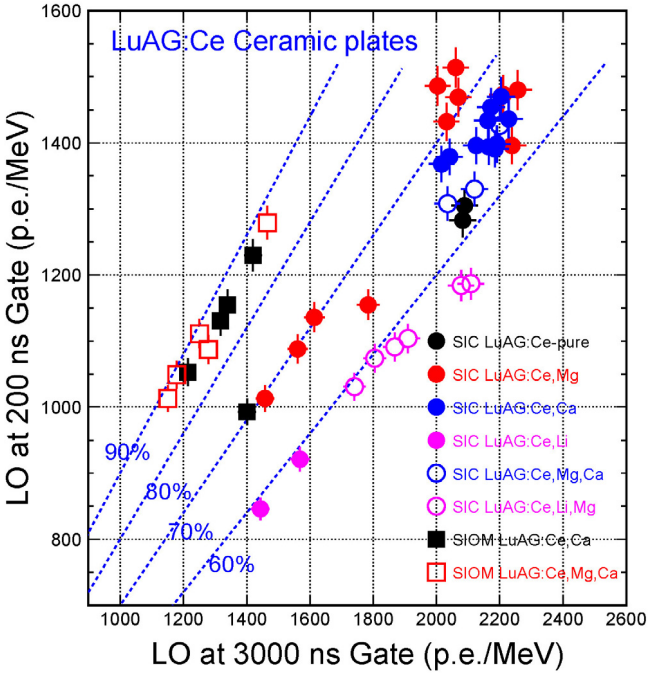

Fig. 17. Correlation between LO in 200 ns and 3000 ns for LuAG:Ce samples with various co-dopings.

Acknowledgment

This work is supported by the U.S. Department of Energy, Office of High Energy Physics program under Award Number DE-SC0011925. Prof. S. Seidel arranged irradiation at the Sandia gamma-ray irradiation facility.

References

[1] A.G. Petrosyan, K.L. Ovanesyan, R.V. Sargsyan, G.O. Shirinyan, D. Abler, E. Auffray, P. Lecoq, C. Dujardin, C. Pedrini, Bridgman growth and site occupation in LuAG:Ce scintillator crystals, J. Cryst. Growth 312 (2010) 3136–3142.

[2] T. Yanagida, Y. Fujimoto, Y. Yokota, A. Yoshikawa, T. Ishikawa, H. Fujimura, H. Shimizu, H. Yagi, T. Yanagitani, Scintillation properties of LuAG (Ce) ceramic and single crystalline scintillator, in: IEEE Nuclear Science Symposuim & Medical Imaging Conference, 2010, pp. 1612–1614.

[3] S. Liu, J.A. Mares, X. Feng, A. Vedda, M. Fasoli, Y. Shi, H. Kou, A. Beitlerova, L. Wu, C. D'Ambrosio, Y. Pan, M. Nikl, Towards bright and fast $Lu_3Al_5O_{12}$:Ce, Mg optical ceramics scintillators, Adv. Opt. Mater. 4 (2016) 731–739.
[4] T. Yanagida, Y. Fujimoto, K. Kamada, D. Totsuka, H. Yagi, T. Yanagitani, Y. Futami, S. Yanagida, S. Kurosawa, Y. Yokota, A. Yoshikawa, M. Nikl, Scintillation properties of transparent ceramic Pr:LuAG for different pr concentration, IEEE Trans. Nucl. Sci. 59 (2012) 2146–2151.
[5] C. Hu, X. Feng, J. Li, L. Ge, Y. Zhang, H. Kou, J. Xu, Y. Pan, Fabrication, optical and scintillation properties of $(Lu_{0.75}, Y_{0.25})$AG:Pr ceramic scintillators, Opt. Mater. 69 (2017) 214–218.
[6] R.-Y. Zhu, A very compact crystal shashlik electromagnetic calorimeter for future hep experiments, J. Phys. Conf. Ser. 928 (2017) 012015.
[7] B. Bilki, C.M.S.C. the, CMS forward calorimeters Phase II Upgrade, J. Phys. Conf. Ser. 587 (2015) 012014.
[8] D.-A. Ma, R.-Y. Zhu, Light attenuation length of barium fluoride crystals, Nucl. Instrum. Methods Phys. Res. A 333 (1993) 422–424.
[9] W. Chewpraditkul, M. Moszynski, Scintillation Properties of $Lu_3Al_5O_{12}$, Lu_2SiO_5 and $LaBr_3$ crystals activated with cerium, Physics Procedia 22 (2011) 218–226.
[10] W. Chewpraditkul, L. Swiderski, M. Moszynski, T. Szczesniak, A. Syntfeld-Kazuch, C. Wanarak, P. Limsuwan, Scintillation Properties of LuAG:Ce, YAG:Ce and LYSO:Ce Crystals for Gamma-Ray Detection, IEEE Trans. Nucl. Sci. 56 (2009) 3800–3805.